

# How to Build Fully $\pi$ -Conjugated Architectures with Thienylene and Phenylene Fragments

Sandrine Lois,<sup>[a]</sup> Jean-Charles Florès,<sup>[a]</sup> Jean-Pierre Lère-Porte,<sup>\*,[a]</sup>  
Françoise Serein-Spirau,<sup>\*,[a]</sup> Joël J. E. Moreau,<sup>[a]</sup> Karinne Miquieu,<sup>\*,[b]</sup>  
Jean-Marc Sotiropoulos,<sup>\*,[b]</sup> Patrick Baylère,<sup>[b]</sup> Monique Tillard,<sup>[c]</sup> and Claude Belin<sup>[c]</sup>

**Keywords:** Sulfur heterocycles / Noncovalent interactions / Photoelectron spectroscopy / Density functional calculations

A series of small-sized model  $\pi$ -conjugated oligomers have been prepared from thienylene and phenylene or dimethyl- or dimethoxy-substituted phenylene units. Crystallographic data for the methoxylated compound show a quasi-planar conformation with a non-covalent S–O interaction. The resulting strong conjugation in the gas phase has also been highlighted by UV/photoelectron spectroscopy and theoretical calculations (DFT). Indeed, for these compounds there is a large energy gap  $\Delta E^{\pi}$  arising from the interaction between the molecular orbitals of the isolated thienylene-phenylene species. This can be explained in terms of the energies of the two  $\pi$  orbitals of the dimethoxyphenylene unit, the shape of these molecular orbitals in a three-orbital interaction diagram and by the presence of the S $\cdots$ O interaction which re-

duces the inter-ring angle between the two aromatic cycles. The nature of the sulfur–oxygen interaction, discussed from a theoretical point of view, is mainly electrostatic, the orbital contribution from the only correctly directed orbitals  $n_{O\sigma}$  and  $\sigma^*_{S-C}$  being slightly stabilising. These results show extensive conjugation of the  $\pi$  system corroborated by a small HOMO–LUMO gap. These studies, carried out in the solid state and in the gas phase, show how important it is to combine thienylene and dialkoxyphenylene fragments to obtain oligomers with a strong electronic delocalisation. Thus, these compounds are of interest in the fields of electronic and optoelectronic devices.

(© Wiley-VCH Verlag GmbH & Co. KGaA, 69451 Weinheim, Germany, 2007)

## Introduction

$\pi$ -Conjugated organic polymers have received much attention for several years because of the large variety of applications directly associated with the existence of an extended conjugated  $\pi$ -system along the polymer backbone. They have attracted much interest in the design of electronic and optoelectronic devices such as organic field-effect transistors (OFET), organic light-emitting diodes (OLED) or solar cells because of their remarkable electronic and electro-optical properties<sup>[1,2]</sup> which are easy to tune as a result of their molecular and supramolecular chemistry. Among the more notable examples, the regioregular poly(3-alkylthiophene) exhibits excellent chain planarity and extended conjugation lengths as a result of its head-to-tail regiochemistry,<sup>[3]</sup> leading to highly conjugated sheets with high field-

effect mobilities.<sup>[4]</sup> More recently, highly regioregular thienylene-2,5-dialkoxyphenylene copolymers have been developed and have shown very interesting properties: the presence of polar dialkoxy chains ensured excellent glass adhesion and enabled the formation of homogeneous thin-film coatings. These materials are highly fluorescent in solution and this fluorescence could be polarised by ordering these polymers by coating them on an oriented Teflon deposit.<sup>[5]</sup> Moreover, very low band gaps and low oxidation potentials were recorded which are indicative of highly conjugated  $\pi$  systems.<sup>[6]</sup> Finally, one such polymer exhibited self-organisation properties leading to lamellar structures with favourable  $\pi$ -stacking interactions between two consecutive conjugated chains characterised by an interchain distance of 3.8 Å.

In the search for novel materials with transport properties resulting from optimised  $\pi$ -conjugation, oligo(phenylenethienylene)s have been developed as a new class of organic semi-conductor.<sup>[7]</sup> Interesting electronic mobilities in organic field-effect transistors formed from this kind of stable and easily processable compound<sup>[8]</sup> have demonstrated that these compounds have extended conjugation. However, building oligo(phenylenethienylene)s consisting of more than five-to-six consecutive rings leads to fairly insoluble compounds and prevents advantage being taken of this extended conjugation. To overcome the solubility problem,

[a] Hétérochimie Moléculaire et Macromoléculaire, UMR CNRS 5076, Ecole Nationale Supérieure de Chimie de Montpellier, 8, rue de l'École Normale, 34296 Montpellier Cedex 05, France  
E-mail: lere@enscm.fr

[b] Equipe de Chimie-Physique, IPREM-UMR CNRS 5254 Avenue de l'Université, B. P. 1155, 64013 Pau Cedex, France  
E-mail: jean-marc.sotiro@univ-pau.fr

[c] Laboratoire des Agrégats Moléculaires et Matériaux Inorganiques, UMR CNRS 5072, Université Montpellier II, 2 Place Eugène Bataillon, 34095 Montpellier Cedex 5, France  
Supporting information for this article is available on the WWW under <http://www.eurjoc.org> or from the author.

alkyl or alkoxy chains can be introduced into the conjugated backbone leading to oligo(2'-thienylene-2,5-dialkoxyphenylene) nanostructures. To improve and better tune the optoelectronic properties of these regioregular alternating sequences of thienylene and 2,5-dialkoxyphenylene moieties and in particular to explore whether such models are potentially interesting as compounds with high field-effect mobilities, it was important to examine if such sequences are appropriate for building fully conjugated chains.

In this work, we have studied the electronic properties of poly(phenylenethienylene) compounds and the effect of phenylene 2,5-disubstitution by alkoxy groups on the conjugation. We focused our attention on understanding the origin of the planarity of these compounds. What is the main factor leading to this planarity? Is it an intrinsic property bestowed by the alkoxy groups or a consequence of the packing effect in the solid state? The answers to these problems could only be found in an experimental study in the gas phase in which the molecular entities are fully isolated from each other. Small-sized thienylene-2,5-disubstituted-phenylene oligomers have been elaborated as models to study by UV/photoelectron spectroscopy (UV/PES) in the gas phase and by density functional calculations (DFT). Analysis of the results obtained in the gas and condensed phases has allowed us to understand the crucial role played by the intramolecular S...O interaction in determining the planarity of these oligomers.

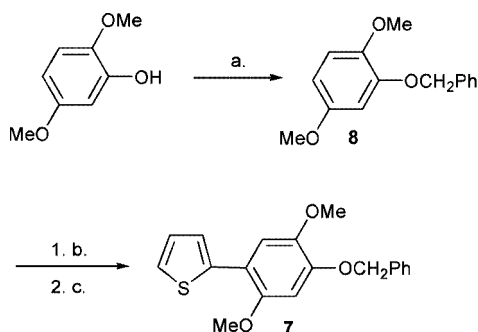
## Results and Discussion

### Synthesis

Seven model compounds containing the thienylene-2,5-disubstituted-phenylene system were elaborated using Stille or the Suzuki palladium(0)-catalysed cross-coupling. Six of them were prepared according to the synthetic pathways described in Scheme 1: equimolar amounts of monobrominated benzene and tributylstannylthiophene for **1–3** (Scheme 1, a) and a half equimolar amount of a dibrominated benzene moiety relative to 2-tributylstannylthiophene for **4–6** (Scheme 1, b).

This general synthetic pathway is efficient and easier to implement than those reported in the literature for some compounds: for instance, phenylthiophene **1** has been prepared via a catalysed palladium(0) Negishi cross-coupling

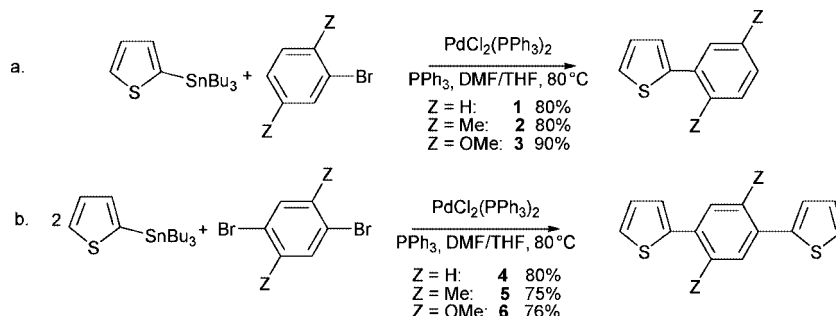
from a sensitive and non-storable thienylzinc chloride intermediate, itself elaborated from the corresponding organolithium derivative and rigorously dried zinc dichloride.<sup>[9]</sup> Concerning the access to **2**, the protocol proposed herein is an efficient alternative to the reaction of thiophene in the presence of a catalytic amount of concentrated sulfuric acid with a *cis/trans* mixture of 3,6-dimethoxy-3,6-dimethylcyclohexa-1,4-diene (ca. 1:1), itself obtained by electrochemical oxidation of *p*-xylene.<sup>[10]</sup> Moreover, the preparative method described herein was very convenient for the preparation of the three-ring compounds **4–6** and avoided the elaboration of specific reactive species such as 2-thienylbis-(isobutyloxy)borane to prepare **4** in 72% yield in a 24 h Suzuki coupling or 2-thienylcadmium chloride, prepared from toxic but more easily dried and stored cadmium chloride, to obtain **5** in 57% yield.<sup>[9]</sup> Finally, **6** was selectively prepared according to Scheme 1, whereas use of 2-thienylzinc chloride in a palladium(0)-catalysed cross-coupling with 1,4-dimethoxybenzene yielded a five-ring byproduct (14%) besides the desired three-ring oligomer synthesised in 49% yield.<sup>[9]</sup> To prepare **7**, 2,5-dimethoxyphenol<sup>[11]</sup> was *O*-alkylated in 93% yield with one equivalent of benzyl bromide in the presence of K<sub>2</sub>CO<sub>3</sub> in refluxing acetonitrile (Scheme 2).<sup>[12]</sup> The obtained 1-benzyloxy-2,5-dimethoxybenzene (**8**) was then selectively iodinated in 86% yield in the 4-position of the phenylene with 1.05 equivalent of *N*-iodosuccinimide activated by 0.3 equivalent of trifluoroacetic acid.<sup>[13]</sup> The resulting 1-benzyloxy-4-iodo-2,5-di-



a. PhCH<sub>2</sub>Br, K<sub>2</sub>CO<sub>3</sub>, CH<sub>3</sub>CN reflux (93%); b. NIS, CF<sub>3</sub>CO<sub>2</sub>H, CH<sub>3</sub>CN (86%);

c.  B(OH)<sub>2</sub>, Pd<sub>2</sub>dba<sub>3</sub>, PPh<sub>3</sub>, Na<sub>2</sub>CO<sub>3</sub>, H<sub>2</sub>O/THF, (71%)

Scheme 2. Synthesis of 1-benzyloxy-2,5-dimethyl-4-(2-thienyl)benzene **7**.



Scheme 1. Synthesis of thienylene-1,4-disubstituted phenylenes **1–6**.

methoxybenzene was immediately treated with 1.2 equivalent of 2-thiopheneboronic acid in a Pd<sup>0</sup>-catalysed Suzuki cross-coupling to afford **7** in 71% yield

The seven thienylene-2,5-disubstituted-phenylene oligomers were isolated as solids except for **2** and **3** which are colourless or light-yellow oils.

### Structural Study in the Solid State by X-ray Diffraction Experiments

After slow recrystallisation from an ethanol/toluene solution, white needle-shaped monocrystals of **6** and **7** were obtained and studied by X-ray diffraction.

The asymmetric unit of **7** consists of one molecule and the orthorhombic  $P2_12_12_1$  unit cell contains four molecules. The  $P2/c$  monoclinic unit cell of **6** also contains four molecules located at inversion centres in such a way that the asymmetric unit consists of two independent half molecules (Figure 1).

C(thiophene)–C(phenylene) bond lengths, distances between the sulfur and the oxygen and the dihedral angles between the thienylene and the phenylene rings have been examined and the recorded values for **6** and **7** are reported in Table 1.

Table 1. X-ray-diffraction determined structural data for **6** and **7**.

	<b>7</b>	<b>6</b> <sub>1</sub>	<b>6</b> <sub>2</sub>
$\Phi$ [°]	5.85	10.49	11.88
$d(\text{C}_{\text{Th}}\text{--C}_{\text{Ph}})$ [Å]	1.459	1.470	1.476
$d(\text{S--O})$ [Å]	2.705	2.700	2.715

As expected, in the two compounds **6** and **7**, the inter-ring C<sub>Th</sub>–C<sub>Ph</sub> bond length reveals a character between a single and a double bond and tends to decrease with the inter-ring torsion angle. The low values of the dihedral angle ( $\Phi$ ) recorded in the crystal state indicate quasi-planar conformations and are the signature of a high level of conjugation between the aromatic rings. Moreover, the observed sulfur–oxygen distances are considerably shorter (2.7 Å) than the sum of the van der Waals radii of sulfur and oxygen (1.85 + 1.5 = 3.35 Å); these observations are consistent with the existence of non-covalent intramolecular sulfur–oxygen interactions (S $\cdots$ O) which induce self-rigidification of the conjugated system in quasi-planar conformations with an extended conjugation. It is worth noting

that the two units **6**<sub>1</sub> and **6**<sub>2</sub> adopt an *anti* conformation in the crystal state, the intramolecular (S $\cdots$ O) interactions being optimised. Such S $\cdots$ O interactions, which are the driving force for the stabilisation of the conjugated segment in the *trans* conformation for the thienylene rings, have been observed in the X-ray crystallographic structure of a variety of oligo(3,4-ethylenedioxythiophene)s.<sup>[14]</sup>

Such S $\cdots$ O interactions have been evidenced in the crystal state of thiazole nucleosides,<sup>[15]</sup> acetazolamide, thiadiazolnethione,<sup>[16]</sup> dimethyl 1,3-dithiolan-2-ylidenemalonate,<sup>[17]</sup> dimethyl 2,2'-bithiophene-3,4'-dicarboxylate, dimethyl 2,2'-bithiophene-3,3'-dicarboxylate<sup>[18]</sup> and extended conjugated systems containing at least two consecutive (3,4-ethylenedioxythiophene) entities.<sup>[14,19]</sup> From radiocrystallographic data, all the authors who observed the intramolecular non-covalent S $\cdots$ O interaction attribute to it the self-rigidification of the molecular structure in a privileged conformation. Since a radiocrystallographic study can be realised with monocrystals of suitable compounds, such intramolecular non-covalent S $\cdots$ O interactions have been evidenced but, to the best of our knowledge, have never been explained. Hence DFT calculations were carried out to provide more information on this interaction. Moreover, in order to understand the role played by the alkoxyphenylene substituent in the observed planarity of **6** and **7** and to avoid the packing effect in the crystal, the calculations were realised considering the compounds as completely individual species, that is, as in the gas phase. Moreover, quantum calculations on model oligomers **1–6** were carried out to gain information on the geometrical properties of the thienylene-2,5-disubstituted-phenylene sequences. Additionally, the electronic properties of these compounds will be consolidated by UV/PES. These properties provide information on the  $\pi$ – $\pi$  orbital interactions, and hence on the magnitude of the conjugation and also on the position of the HOMO orbital which can be correlated with the oxidation potential.

### Quantum Chemical Study in the Gas Phase

The  $\pi$ – $\pi$  interactions in the gas phase between the thienylenes and phenylenes moieties were first determined in the smaller systems **1–3** and then this study was extended to systems substituted by one more thienylene ring **4–6** (Scheme 3).

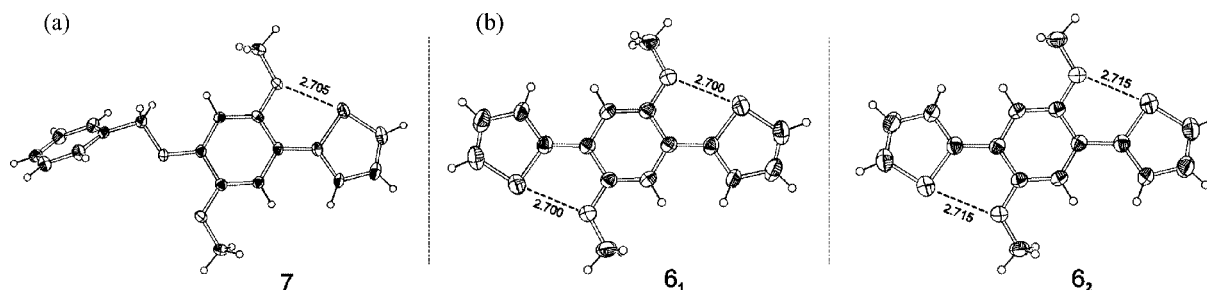
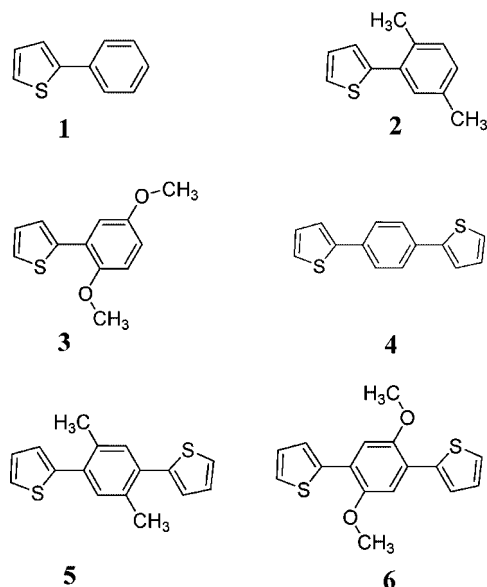


Figure 1. ORTEP diagrams of (a) **7** and (b) **6**. Intramolecular S $\cdots$ O interactions are indicated by dotted lines.



Scheme 3. Privileged conformations of compounds 1–6 studied in the gas phase.

### Structural Study of the Two-Ring Compounds

For compounds 1–3, calculations with the B3LYP hybrid functional and the 6-31G(d,p) basis set were carried out (see the Theoretical Section in the Experimental Section). The privileged conformers are presented in Scheme 3 and the geometrical parameters are reported in Table 2. For 1, only one conformer exists on the potential energy surface. The two rings are slightly twisted with a 28.5° inter-ring angle  $\Phi$  and the  $C_{\text{Th}}-C_{\text{Ph}}$  bond length of about 1.47 Å is between a single and a double bond. In contrast, two rotamers were found on the potential energy surface for 2, but with no significant energy gap (0.43 kcal mol<sup>-1</sup>). The more stable rotamer corresponds to the arrangement with the lower steric hindrance (see Supporting Information for the other rotamer). The angle between the two units is the highest observed (41.5°) for these compounds. For 3, the global minimum (for all the other rotamers see the Supporting Information) adopts a conformation with a short S...O distance of 2.798 Å, less than the sum of the van der Waals radii, and has the smallest inter-ring angle of 24.2°. The  $C_{\text{Th}}-C_{\text{Ph}}$  bond length is 1.470 Å, similar to that observed for 1 and 2, and consequently does not seem to provide much information on the inter-ring conjugation.

Table 2. Geometrical parameters for 1–6.

Compound	1	2	3	4	5	6
$d(C_{\text{Th}}-C_{\text{Ph}})$ [Å]	1.469	1.475	1.470	1.466	1.473	1.467
$\Phi$ [°]	-28.5	-41.5	-24.2	26.2	-39.7	-21.1
$d(S\cdots O)$ [Å]	–	–	2.798	–	–	2.786
$q_{\text{S}}^{\text{[a]}}$	0.45	0.45	0.49	0.45	0.45	0.49
$q_{\text{X}}^{\text{[a]}}$	0.24	0.24	-0.53	0.24	0.24	-0.53

[a] Total natural charges from the NBO analysis:  $q_{\text{S}}$ : charge on sulfur;  $q_{\text{X}}$ : charge on hydrogen or oxygen (facing the sulfur atom).

### Structural Study of the Three-Ring Compounds

The geometrical parameters for 4–6 computed by the DFT method are presented in Table 2. Compound 6 adopts a privileged conformation with a short S...O distance (2.786 Å) and the two oxygen lone-pairs point towards the sulfur (Scheme 3), in agreement with the experimental crystallographic data. The main result of this study is the change in the inter-ring angles upon substitution of the phenyl ring and the lengthening of the conjugated skeleton. The addition of a thienylene entity onto a phenylene-thienylene fragment leads to a decrease in the inter-ring angle. Moreover, as previously observed in the two-ring series, the smallest inter-angle value in the three-ring series is obtained for the dimethoxylated compound 6 (21.1°). These geometrical parameters determined in the gas phase are in quite good agreement with the theoretical parameters previously reported by Pan et al.<sup>[20]</sup> at the HF/3-21G\* level. However, for these three compounds, the inter-ring angles determined by DFT are smaller than those determined by HF calculations because electronic correlation is taken into account in the DFT, but not in the HF calculations.

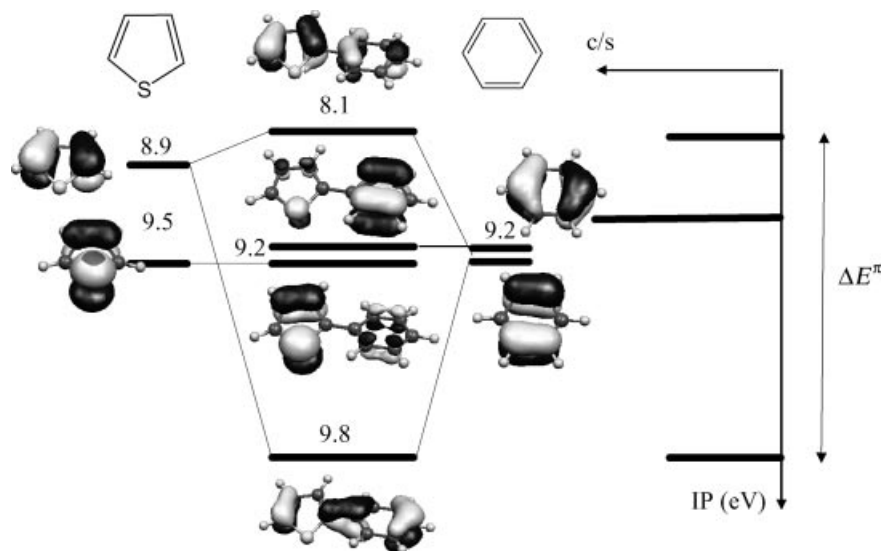
### UV/Photoelectron Spectroscopic Study in the Gas Phase

UV/photoelectron spectroscopy has proved to be an excellent experimental tool for revealing the electronic structure and bonding features of molecules.<sup>[21]</sup> In the present study of these  $\pi$ -conjugated systems, this spectroscopic method can provide an evaluation of the effect of the phenylene substituents (H, CH<sub>3</sub>, OCH<sub>3</sub>) on the electronic properties of the thienylene-phenylene compounds. Experimentally, thanks to UV/photoelectron spectroscopy, the position of the HOMO orbital can be obtained as well as information on the  $\pi$ - $\pi$  splitting ( $\Delta E^{\pi}$ ) which corresponds to the magnitude of the interaction. This latter value depends on the orbital overlap, but also on the energies of the isolated fragments. So, if we consider the experimental energies of the  $\pi$  orbitals of the phenylene fragments<sup>[22]</sup> (benzene:  $\pi^{\text{Ph}_1}$ ,  $\pi^{\text{Ph}_2}$ : 9.2 eV; dimethylbenzene:  $\pi^{\text{Ph}_1}$ : 8.6 eV,  $\pi^{\text{Ph}_2}$ : 9.2 eV; dimethoxybenzene:  $\pi^{\text{Ph}_1}$ : 7.9 eV,  $\pi^{\text{Ph}_2}$ : 9.2 eV), they are quite close to the  $\pi$  orbitals of thiophene [ $\pi^{\text{Th}_1}$ : 8.9 eV and  $\pi^{\text{Th}_2}$  ( $n_{\text{S}\pi}$ ): 9.2 eV].<sup>[23]</sup> Consequently, the  $\pi$ - $\pi$  interactions between these two types of units are expected to be strong. Scheme 4 shows in a simple way the correlation between the orbital interactions of the isolated fragments and the corresponding photoelectron spectrum.

### Electronic Properties of the Two-Ring Compounds

The photoelectron spectra were recorded at 40 °C for 1 and at 120 °C for 2 and 3 ( $p = 10^{-5}$  mbar, beam temperature).

The photoelectron (PE) spectrum of 1 (Figure 2) exhibits three well-resolved bands at 8.1, 9.2 and 9.8 eV and then broad bands between 11.4 and 15 eV. Considering the experimental ionisation potentials (IP) of the two fragments benzene<sup>[22]</sup> and thiophene,<sup>[23]</sup> the first IP of 1 (8.1 eV) suggests a strong interaction between the  $\pi$  systems of the two



Scheme 4. Schematic  $\pi$ - $\pi$  interactions ( $\Delta E^\pi$ ) illustrated for phenylthiophene **1** with experimental ionisation energies in eV. The corresponding photoelectron spectra are qualitatively simulated.

rings. From such considerations, this spectrum can be easily described with a two-orbital interaction diagram: the first and the third bands are assigned to the ejection of electrons localised in the molecular orbitals (MO) resulting from the interaction between the  $\pi^{\text{Ph}_1}$  and  $\pi^{\text{Th}_1}$  orbitals since only the  $\pi^{\text{Ph}_1}$  orbital possesses electron density on the carbon atom linked to the thienyl ring (Scheme 4). These orbitals correspond to the  $\pi^-$  (out-of-phase) and  $\pi^+$  (in-phase) combination of orbitals, respectively, and are named  $\pi_1^1$  and  $\pi_4^1$ . The middle band, more intense, is associated with two ionisations from the  $\pi^{\text{Ph}_2}$  and  $\pi^{\text{Th}_2}$  orbitals. For this compound, the experimental  $\Delta E^\pi$  is about 1.7 eV and is in perfect accord with the theoretical value (1.7 eV).

These semi-empirical assignments were confirmed by determination of the Kohn–Sham energies, the nature of the Kohn–Sham orbitals (KS) and the estimated vertical ionisation energies (see Supporting Information for the Kohn–Sham energies and Figure 2 for a plot of the Kohn–Sham orbitals and the estimated vertical ionisation energies).

When methyl or methoxy substituents are introduced into the benzene ring the PE spectra are modified. In the case of **2**, two intense bands appear at 8.6 and 9.1 eV, with two shoulders at about 8.2 and 9.4 eV (Figure 3), whereas the spectrum of **3** displays a different shape with five sharp peaks below 10.5 eV (7.6, 8.3, 8.9, 9.5 and 10.1 eV) and a massif between 11 and 16 eV (Figure 4).

A more complex interaction diagram arises from phenyl substitution (Figure 5). Indeed, the two  $\pi$  orbitals of the aryl group  $\pi^{\text{Ph}_1}$  and  $\pi^{\text{Ph}_2}$  are localised on the carbon atom linked to the thienylene cycle and not only  $\pi^{\text{Ph}_1}$ , as observed for the phenyl group. Consequently, the  $\pi^{\text{Th}_1}$  orbital interacts with the  $\pi^{\text{Ph}_1}$  and  $\pi^{\text{Ph}_2}$  orbitals of the phenylene group, inducing better delocalisation on three orbitals [ $\pi^{x_1}$ ,  $\pi^{x_2}$ ,  $\pi^{x_4}$  with  $x = 2$  (Me) or 3 (OMe)] instead of two as in **1** ( $\pi_1^1$ ,  $\pi_4^1$ ). In this way, for **2** and **3**, we estimate the  $\pi$ - $\pi$  interaction by considering the out-of-phase and in-phase combinations ( $\pi^{x_1}$  and  $\pi^{x_4}$ ), as for **1**.

For **2**, the experimental  $\Delta E^\pi$  is only about 1.2 eV and corresponds to the energy gap between the ionisations represented by the two shoulders at 8.2 and 9.4 eV. The nature of the others ionisations are presented under the spectrum in the Supporting Information. Conversely, the replacement of hydrogen by a methoxy group in the same positions, leads to a lowering of the first IP and to an increase in  $\Delta E^\pi$ . Plots of the first, second and fourth MOs clearly show a mixing between the two  $\pi$  orbitals of the dimethoxybenzene and the  $\pi^{\text{Th}_1}$  orbital of the thiophene. In this case, the experimental  $\Delta E^\pi$ , which corresponds to the difference between the first and fourth bands, is about 1.9 eV and agrees with the theoretically determined value (2.1 eV). Among the values of  $\Delta E^\pi$  recorded for compounds **2** and **3**, the methoxy disubstitution at the 2,5-positions of the phenylene contributes to an enhancement of the  $\pi$ - $\pi$  interaction between the phenylene and the thienylene fragments.

In order to understand why this  $\pi$ - $\pi$  gap is maximal in **3**, we examined the two factors that influence  $\Delta E^\pi$ , the energy difference between the involved orbitals of the two isolated fragments and the through-space orbital overlap, which depends on the dihedral angle  $\Phi$  between the two rings. To estimate the incidence of the proximity of the energy levels of the isolated fragments, the same torsion angle  $\Phi$  between the two rings was imposed and  $\Delta E^\pi$  for compounds **1**–**3** (Table 3) were then compared. For the same inter-ring torsion angle  $\Phi$  (0, 45, 135 or 180°), for compounds **1** and **2**  $\Delta E^\pi$  is the same and varies in the same way when  $\Phi$  is modified. In contrast, for **3** the  $\Delta E^\pi$  value is always higher than those for **1** and **2**. This means that the difference between the energies of the isolated fragments has an important effect on the  $\Delta E^\pi$  splitting. In fact, the highest  $\Delta E^\pi$  value observed for **3** can be ascribed to the energy of the  $\pi^{\text{Ph}_1}$  orbital [ $\pi^{\text{Ph}_1}$  for dimethoxybenzene (−5.31 eV) is higher in energy than  $\pi^{\text{Ph}_1}$  for dimethylbenzene (−6.14 eV) and  $\pi^{\text{Ph}_1}$  for benzene (−6.72 eV)] and also to the involvement of the  $\pi^{\text{Ph}_2}$  orbital in this interaction (see Supporting Information

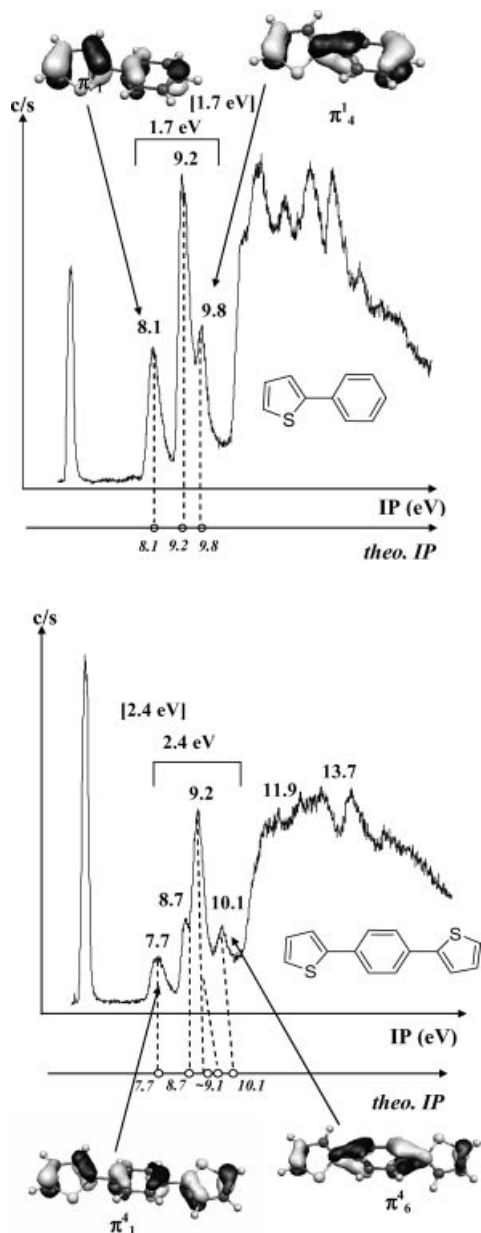


Figure 2. Photoelectron spectra of **1** and **4**. Experimental and theoretical (*italics*) IP [eV] values, experimental and theoretical (in brackets)  $\Delta E^\pi$  values [eV], with  $\Delta E^\pi$  being the energy difference between the MOs involved in the  $\pi$ - $\pi$  interaction. MOLEKEL plots of the orbitals involving in the  $\pi$ -delocalisation are shown.

for the Kohn–Sham orbital energies and Figure 5). These energetic positions lead to better delocalisation.

Concerning the effect of the dihedral angle, the small value calculated for the inter-ring torsion angle  $\Phi$  for **3** (24.2°), compared with those calculated for **1** (28.5°) and **2** (41.5°), also contributes to an enhanced splitting  $\Delta E^\pi$ . The results presented in Table 3 clearly show that for **1** and **2** the geometry of the structure that undergoes  $\pi$ -orbital overlap is the main factor influencing the magnitude of  $\Delta E^\pi$  and consequently that of the conjugation: indeed, the highest inter-ring angle observed for **2** (41.5°) is probably a result of the steric effect of the methyl substituents and corre-

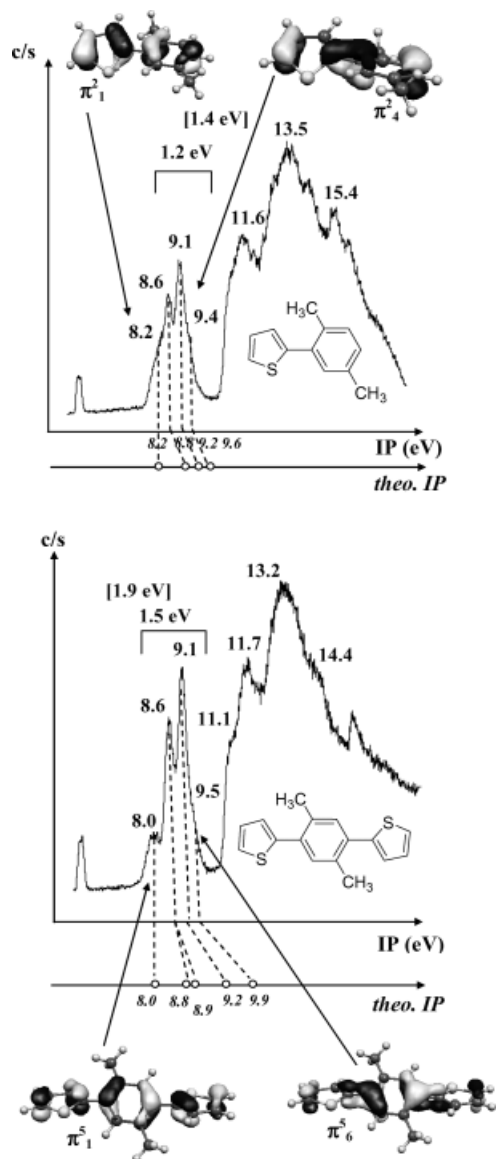


Figure 3. Photoelectron spectra of **2** and **5**. Experimental and theoretical (*italics*) IP [eV] values, experimental and theoretical (in brackets)  $\Delta E^\pi$  values [eV], with  $\Delta E^\pi$  being the energy difference between the MOs involved in the  $\pi$ - $\pi$  interaction. MOLEKEL plots of the orbitals involving in the  $\pi$ -delocalisation are shown.

Table 3. Experimental and theoretical  $\Delta E^\pi$  values for the privileged conformers. Theoretical  $\Delta E^\pi$  values for the other conformers ( $\Phi = 0, 180, 45, 135^\circ$ ).

	<b>1</b> $\Phi = 28.5^\circ$	<b>2</b> $\Phi = 41.5^\circ$	<b>3</b> $\Phi = 24.2^\circ$
$\Delta E^\pi_{\text{exp.}}$ [eV]	1.7	1.2	1.9
$\Delta E^\pi_{\text{theo.}}$ [eV]	1.7	1.4	2.1
$\Phi = 0, 180^\circ$			
$\Delta E^\pi_{\text{theo.}}$ [eV]	1.9	1.9	2.2
$\Phi = 45, 135^\circ$			
$\Delta E^\pi_{\text{theo.}}$ [eV]	1.4	1.4	1.8

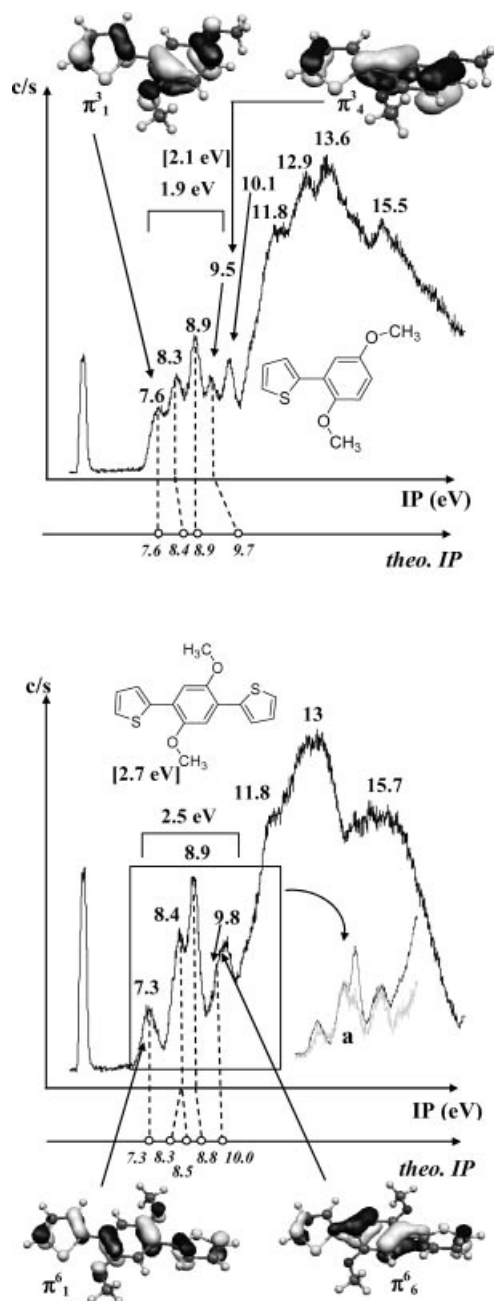


Figure 4. Photoelectron spectra of **3** and **6**. Experimental and theoretical (*italics*) IP [eV] values, experimental and theoretical (in brackets)  $\Delta E^\pi$  values [eV], with  $\Delta E^\pi$  being the energy difference between the MOs involved in the  $\pi$ - $\pi$  interaction. MOLEKEL plots of the orbitals involving in the  $\pi$ -delocalisation are shown. (a) Superposition of the He(II) (grey) and He(I) (black) spectra of the frame part.

sponds to the smallest  $\Delta E^\pi$  (1.2 eV experimental and 1.4 eV theoretical). For **3**, if we compare the relative stabilities of the more probable conformers, the global energy minimum is not for the conformer in which the sulfur and oxygen atoms are in opposite positions ( $\Phi = 25.6^\circ$ ), but in which the methoxy group is directed towards the sulfur ( $\Phi = 24.2^\circ$ ). Consequently, the presence of a non-covalent S $\cdots$ O attractive interaction seems to reduce the dihedral angle between the two rings.

Another parameter that gives information on the delocalisation over the molecular structure is the HOMO–LUMO gap. The energy gap between the two frontier orbitals, summarised in Table 4, gives a rough estimate of the lowest electronic excitation energy. In the UV/Vis spectra an absorption is identified as a  $\pi$ - $\pi^*$  transition. It is noteworthy that the smallest HOMO–LUMO gap is calculated for **3** and it corresponds to the highest absorption wavelength maximum ( $\lambda_{\max}$ ). The destabilisation of the HOMO, associated with the lowest ionisation potential for **3** (7.6 eV for **3** vs. 8.1 eV for **1** and 8.2 eV for **2**), leads to the smallest HOMO–LUMO gap which makes easier the electron transfer.

Table 4. Experimental and theoretical  $\Delta E^\pi$ ,  $\Delta E(\text{HOMO-LUMO})$  and absorption wavelength maxima  $\lambda_{\max}$ .

	<b>1</b>	<b>2</b>	<b>3</b>	<b>4</b>	<b>5</b>	<b>6</b>
$\Delta E^\pi_{\text{exp.}}$ [eV]	1.7	1.2	1.9	2.4	1.5	2.7
$\Delta E^\pi_{\text{theo.}}$ [eV]	1.7	1.4	2.1	2.4	1.9	2.7
$\Delta E(\text{H-L})_{\text{theo.}}$ [eV]	4.8	4.9	4.4	4.0	4.3	3.7
$\lambda_{\max}$ [nm]	285	275	315	325	294	358

In summary, by considering the value of  $\Delta E^\pi$ , corresponding to the HOMO–HOMO-3 gap and related to the  $\pi$  conjugation as well as the HOMO–LUMO gap, disubstitution in the 2,5-positions by methoxy groups leads to a more delocalised system in the gas phase. Moreover, this low IP (high energy of the HOMO) corresponds to a low oxidation potential.

#### Electronic Properties of the Three-Ring Compounds

In order to see if the previous results can be generalised when the conjugated chain is lengthened by the addition of a thienylene group in the 4-position of the phenylene moiety, we studied **4–6** in the gas phase. For these compounds, the PE spectra (Figure 2, Figure 3 and Figure 4) were recorded between 170 and 180 °C ( $p = 10^{-5}$  mbar, beam temperature) and present similar shapes. The photoelectron spectrum of compound **4** displays a first broad and small band at 7.7 eV separated from the next two recorded at 8.7 and 9.2 eV, respectively, the latter one being intense. The fourth broad but small band is at 10.1 eV.

The same spectral shape arises from **5**. In this case, the first band is shifted towards a higher ionisation potential (8 eV). The positions of the second and third bands are quasi-unchanged (8.6 and 9.1 eV, respectively). The fourth band (9.5 eV) emerges as a shoulder of the third intense band at 9.1 eV.

The spectrum of **6** shows similar band intensities. The first ionisation potential is the smallest IP observed for the six studied models and appears at 7.3 eV. The second IP is recorded at 8.4 eV, the third is an intense band at 8.9 eV and the fourth a weaker and broader one at 9.8 eV.

Analysis of the experimental and theoretical results allowed us to assign the different bands in the PE spectra. For **4** and **5** the ionisations that arise from the removal of an electron from the  $\pi$  orbitals delocalised over the three rings can be assigned to the first and fourth bands (respec-

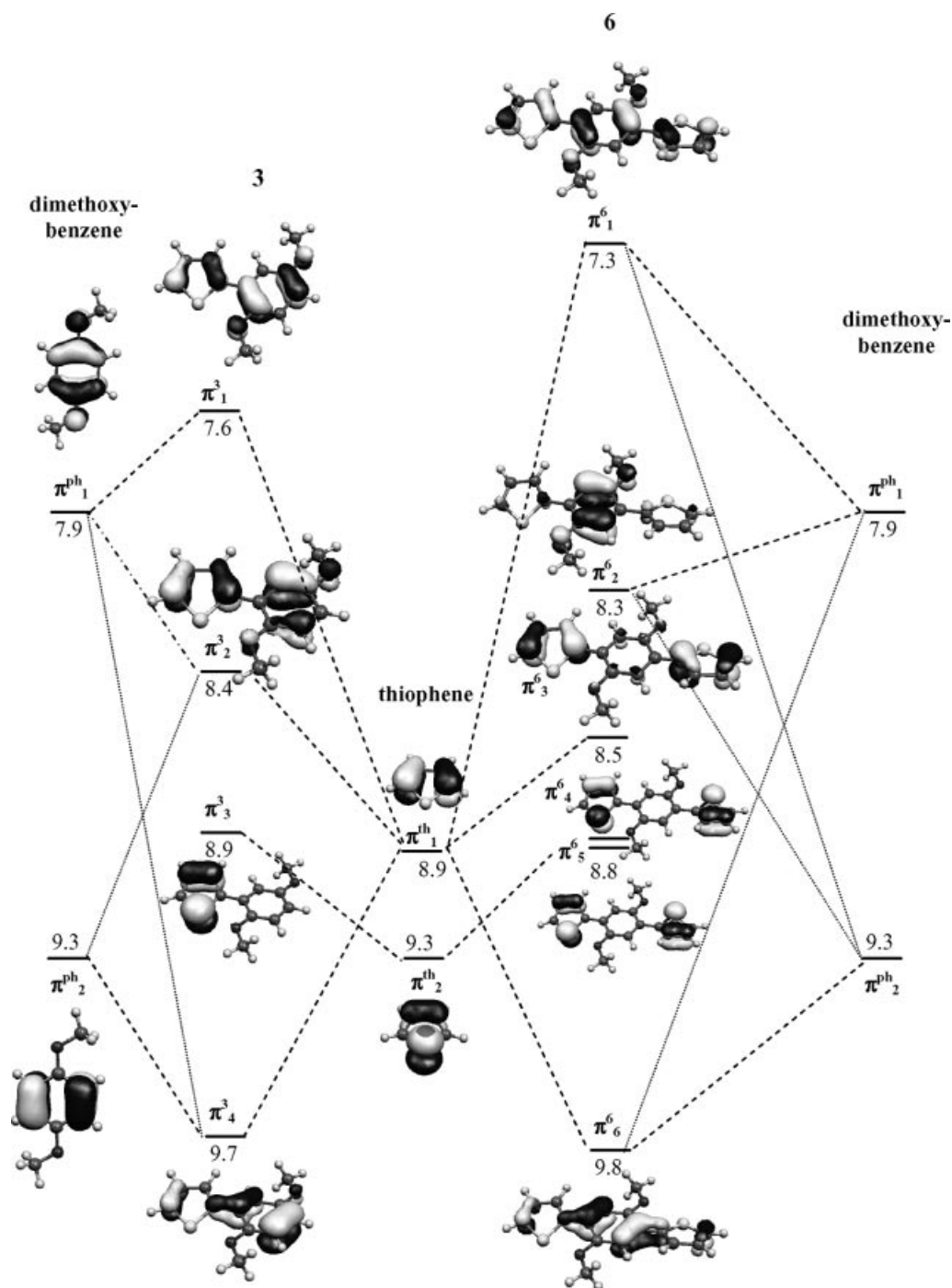


Figure 5. Interaction diagram for **3** and **6**. The main interactions are presented as bold dotted lines and secondary ones as grey dotted lines. Estimated ionisation energies [eV] are shown.<sup>[38]</sup>

tively, 7.7 and 10.1 eV for **4** and 8.0 and 9.5 eV for **5**). For the second and third bands the assignments are presented under the figures in the Supporting Information. As previously observed in the two-ring series, the experimental value of  $\Delta E^\pi$  for the dimethylated compound **5** of about 1.5 eV is smaller than that of the unsubstituted phenyl compound **4** (2.4 eV).

The highest  $\Delta E^\pi$  is observed for **6** and is about 2.5 eV. It is in very good agreement with the theoretical value and corresponds to the energy difference between the first and

the fourth bands, respectively, at 7.3 and 9.8 eV. These bands arise from ionisations of  $\pi$  orbitals delocalised over the thienylene and phenylene units. In this case, for symmetry reasons, only the antibonding  $\pi_1^{\text{Th}}$  orbital can interact with the  $\pi$  phenylene orbitals. Here again, the MO plot (Figure 5) clearly shows that the first, second and sixth orbitals arise from mixing of the  $\pi_1^{\text{Th}}/\pi_1^{\text{Ph}}$  and  $\pi_2^{\text{Ph}}$  orbitals. In contrast, the second band at 8.4 eV and the third one at 8.9 eV represent ionisations from orbitals localised only on the thienylene or the phenylene rings (see the MO plot un-

der the spectrum in the Supporting Information). He(I)/He(II) changes are in agreement with the proposed interpretations of the spectra. Indeed, it is well known that the relative intensity of bands assigned to molecular orbitals with substantial participation of the sulfur lone-pair decrease in an He(II) spectra.<sup>[24]</sup> To illustrate these modifications, the superimposed He(I) and He(II) photoelectron spectra are presented in Figure 4a for **6** and clearly show the important decrease in the intensity of the third band (8.9 eV), indicative of the participation of sulfur 3s/3p atomic orbitals in the  $\pi$  molecular orbitals concerned.

Comparing the two series of compounds, the lengthening of the conjugated chain leads to a decrease in the first ionisation potential of around 0.4 eV and a more significant splitting  $\Delta E^\pi$  for **4–6**, corresponding to the  $\pi_1$ – $\pi_6$  gap, than that recorded for **1–3**, corresponding to the  $\pi_1$ – $\pi_4$  gap (Figure 2–Figure 4). This result is consistent with enhanced  $\pi$  conjugation in the thienylene-phenylene-thienylene compounds compared with that observed in the thienylene-phenylene ones. Moreover, the greatest  $\Delta E^\pi$  gap and the smallest HOMO–LUMO gap (3.70 eV calcd. for **6** vs. 4.04 eV for **4** and 4.32 eV for **5**) are observed when the phenyl ring is substituted by methoxy groups. These HOMO–LUMO gaps agree with the measured maximum absorption wavelength (Table 4) and are coherent with the fact that **6** is the more delocalised  $\pi$  system.

In summary, the six PE spectra suggest that  $\pi$  conjugation takes place in all the compounds and is greater in the dimethoxylated compounds **3** and **6** than in the unsubstituted **1** and **4** or in the dimethylated compounds **2** and **5**, as shown by the splittings of the  $\pi^+$  and  $\pi^-$  ionisation bands and the  $\Delta E(\text{HOMO–LUMO})$  gaps. Moreover, for **3** and **6** the first IP is the weakest observed; they correspond to the lowest oxidation potentials. All these parameters indicate that dimethoxyphenylene-thienylene sequences are highly  $\pi$ -conjugated systems. Consequently, the strong  $\pi$  conjugation observed in the gas phase for **3** and **6** seems to be mainly due to an intrinsic property of the compounds.

### Character of the S $\cdots$ O Interaction

We previously demonstrated the importance of the presence of 2,5-dialkoxy substituents on phenylene for obtaining highly conjugated systems with small inter-ring angles, strong  $\pi$  delocalisation and small HOMO–LUMO gaps. The presence of the non-covalent S $\cdots$ O interaction observed in isolated molecules **3** and **6** seems to be of great importance. Other authors have investigated by theoretical methods the intramolecular interactions between chalcogen and oxygen or chlorine atoms in systems other than thienylene-phenylene sequences.<sup>[25–28]</sup> These authors explained such types of interaction either by orbital and/or electrostatic interactions. Which factor makes the main contribution in our specific case? To answer this we determined the total natural charges on compounds **1–6** coming from an NBO analysis of the more stable conformers (Table 2). We also investigated the stabilising interaction involving

only the  $\sigma$  oxygen lone-pair by a second-order perturbation theory analysis (NBO calculation).

The atomic charges on the S and O atoms in **3** and **6** are, respectively, 0.49 and –0.53 and suggest, for the S $\cdots$ O interaction, a significant electrostatic interaction between a positively charged S atom and a negatively charged O atom. This is in agreement with the short calculated S $\cdots$ O distance. This electrostatic interaction probably leads to the good planarity of these compounds. Conversely, for **2** and **5**, the atomic charges on the S and H atoms are positive, at 0.45 and 0.24, respectively, and so repulsive. Considering the orbital interaction, the calculated stabilising energies reveal that the interaction between the two correctly directed  $n_{\text{O}}^\sigma$  and  $\sigma_{\text{S–C}}^*$  orbitals is weak (2–3 kcal/mol) and so it would make a slight contribution to the stabilisation of the S $\cdots$ O interaction.

### Conclusions

To build fully  $\pi$ -conjugated architectures it is important to elaborate an alternating sequence of thienylene and 2,5-dialkoxyphenylene entities: a high inter-ring conjugation, which occurs from such a combination, is revealed by a small  $\pi$ – $\pi^*$  gap and a high experimental  $\Delta E^\pi$  between the  $\pi$  orbitals delocalised over the two thienylene and 2,5-dialkoxyphenylene fragments of **6**. The small HOMO–LUMO gap, which leads to an absorption in the visible spectrum, is mainly due to a high HOMO level which induces a small oxidation potential. The very high value of  $\Delta E^\pi$  is due, on the one hand, to the energies and shape ( $\pi_1^{\text{Ph}}$  and  $\pi_2^{\text{Ph}}$  are localised on the carbon linked to the thienylene group close to  $\pi_1^{\text{Th}}$ ) of the isolated fragments and, on the other hand, to the presence of an S $\cdots$ O interaction which favours a small dihedral angle between the two rings and consequently a good  $\pi$ -orbital overlap. In these systems, this intramolecular attractive non-bonding S $\cdots$ O interaction seems essentially of electrostatic nature even if a weak negative hyperconjugation  $n_{\text{O}}^\sigma \rightarrow \sigma_{\text{S–C}}^*$  probably contributes to the interaction. It is noteworthy that non-substituted or 2,5-dialkoxy-substituted thienylene-phenylenes have very closed geometric and electronic characteristics. In contrast to alkyl chains which confer solubility but damage conjugation, the alkoxy substituents provide good solubility and improve the inter-ring conjugation.

Moreover, between such planar nanostructures, intermolecular  $\pi$ -stacking interactions will be particularly favoured and this type of arrangement favours superior transport properties in organic materials resulting in, for example, high field-effect mobilities that can be exploited for use in organic transistors or photovoltaic cells. In addition, the importance of the association of the thienylene and 2,5-dialkoxyphenylene moieties clearly appears to lead, even for very short oligomers, to relatively high absorption maxima and so one can envisage, with longer analogous oligomers, their application in optoelectronic devices such as electroluminescent diodes or solar cells.

## Experimental Section

**General Procedures:** DMF, THF, CH<sub>3</sub>CN and toluene were dried and distilled under nitrogen prior to use. Bromobenzene, benzyl bromide 1-bromo-2,5-dimethylbenzene, 1-bromo-2,5-dimethoxybenzene, 1,4-dibromobenzene, 1,4-dibromo-2,5-dimethylbenzene, 1,4-dibromo-2,5-dimethoxybenzene, 2-tributylstannylthiophene, 2-thiopheneboronic acid, *N*-iodosuccinimide, triphenylphosphane, bis(triphenylphosphane)dichloropalladium, (dibenzylideneacetone)palladium were purchased (Alfa and Aldrich) and used without further purification. <sup>1</sup>H and <sup>13</sup>C NMR spectra were recorded with a Bruker AC 200 spectrometer. Chemical shifts (in δ units, ppm) are referenced to TMS using CHCl<sub>3</sub> (δ = 7.27 ppm) and CDCl<sub>3</sub> (δ = 77.70 ppm) as the internal standards, respectively, for <sup>1</sup>H and <sup>13</sup>C NMR spectra. IR spectra were recorded with a Perkin-Elmer 1000 spectrophotometer and absorption spectra with a Hewlett-Packard 8453 spectrophotometer. Melting points were measured with an Electrothermal 9100 apparatus. Mass spectrometry was carried out with a JEOL JMS-DX 300 apparatus in FAB<sup>+</sup> ionisation mode. C,H elemental analyses were performed by the Service Central d'Analyses du CNRS (Vernaison, France).

The photoelectron spectra were recorded with a Perkin-Elmer 0018 instrument equipped with a 127° cylindrical analyser and analysed using a microcomputer supplemented with a digital analogue converter. The spectra were calibrated using the known autoionisation of helium at 4.99 eV [He(II)/He(I)] and xenon ionisations at 12.13 and 13.44 eV. All the products were vaporised by the heat of the beam. Consequently, the different temperatures presented in this publication correspond to the beam temperature and not the sample temperature. We maintained a stable temperature of the beam in order to vaporise enough of the compounds and to obtain intense spectra.

**2-Phenylthiophene (1):** In a 250 mL round-bottomed flask, bromobenzene (30 mmol, 4.710 g), 2-tributylstannylthiophene (30 mmol, 11.195 g), bis(triphenylphosphane)dichloropalladium (421 mg, 2 mol-%) and triphenylphosphane (1.26 g, 4.8 mmol, 16 mol-%) were introduced under nitrogen into an anhydrous solvent mixture (THF/DMF, 1:1, 60 mL). The medium was stirred at 80 °C for 18 h and treated, after removing THF, with 250 mL of an ammonium fluoride solution (3 M) and diethyl ether (250 mL). The mixture was vigorously stirred for 1 h, and the organic phase was extracted with diethyl ether (3 × 50 mL), filtered, washed with ammonium fluoride solution (50 mL) and then with a saturated sodium chloride solution (50 mL). After drying over sodium sulfate, it was concentrated and the orange liquid was distilled under vacuum to give phenylthiophene as a white bright solid in 80% yield (3.84 g). M.p. 34–36 °C; Eb<sub>(5 × 10<sup>-2</sup>)</sub> 57 °C. <sup>1</sup>H NMR (200 MHz, CDCl<sub>3</sub>): δ = 7.66 (d, *J* = 7.8 Hz, 2 H, H<sub>Th</sub>), 7.43–7.28 (m, 5 H, H<sub>Ph</sub>), 7.11 (dd, *J* = 3.6, *J* = 5.0 Hz, H<sub>Th</sub>) ppm. <sup>13</sup>C NMR (200 MHz, CDCl<sub>3</sub>): δ = 144.9 (C<sub>Th</sub>), 134.9 (C<sub>Ph</sub>), 129.3 (C<sub>Ph</sub>), 128.4 (C<sub>Ph</sub>), 127.9 (C<sub>Th</sub>), 126.4 (C<sub>Ph</sub>), 125.2 (C<sub>Th</sub>), 123.5 (C<sub>Th</sub>) ppm. IR (KBr): ν̄ = 3073, 1680, 1601, 1489, 1447, 1377, 1257, 850, 826, 755, 693 cm<sup>-1</sup>. MS (FAB<sup>+</sup>): *m/z* (%) = 160 [M]<sup>+</sup>. Absorption (CHCl<sub>3</sub>): λ<sub>max</sub> = 285 nm.

The spectroscopic data agree with those reported in the literature.<sup>[9,29]</sup>

**2-(2,5-Dimethylphenyl)thiophene (2):** Compound **2** was prepared according to the same procedure as **1** with 2-bromo-*p*-xylene (16 mmol, 2.96 g), 2-(tributylstannyl)thiophene (16 mmol, 5.970 g), bis(triphenylphosphane)dichloropalladium (224 mg, 2 mol-%) and triphenylphosphane (672 mg, 2.56 mmol) under nitrogen in an anhydrous solvent mixture (THF/DMF, 1:1, 30 mL). After the reaction, the crude product was purified through a chromatographic

silica gel column (pentane/diethyl ether, 90:10) to give **2** as a colourless oil in 80% yield (2.405 g). <sup>1</sup>H NMR (200 MHz, CDCl<sub>3</sub>): δ = 7.32 (dd, *J* = 5, *J* = 1.4 Hz, 1 H, H<sub>Th</sub>), 7.23–7.03 (m, 5 H, H<sub>Th</sub> + H<sub>Ph</sub>), 2.37 (s, 3 H, H<sub>Me</sub>), 2.34 (s, 3 H, H<sub>Me</sub>) ppm. <sup>13</sup>C NMR (200 MHz, CDCl<sub>3</sub>): δ = 143.4 (C<sub>Th</sub>), 135.4 (C<sub>Ph</sub>), 134.0 (C<sub>Ph</sub>), 133.0 (C<sub>Ph</sub>), 130.9 (C<sub>Th</sub>), 130.7 (C<sub>Th</sub>), 128.9 (C<sub>Th</sub>), 127.9 (C<sub>Ph</sub>), 126.3 (C<sub>Ph</sub>), 125.0 (C<sub>Ph</sub>), 20.7 (C<sub>Me</sub>), 20.6 (C<sub>Me</sub>) ppm. IR (KBr): ν̄ = 3107, 3070, 3015, 2952, 2915, 2865, 1728, 1612, 1496, 1437, 1379, 1254, 1220, 1168, 1041, 888, 833, 810, 696, 602, 557 cm<sup>-1</sup>. MS (FAB<sup>+</sup>): *m/z* (%) = 189 (60) [M + 1]<sup>+</sup>, 149 (90). Absorption (CHCl<sub>3</sub>): λ<sub>max</sub> = 270 nm.

The spectroscopic data agree with those reported in the literature.<sup>[10]</sup>

**2-(2,5-Dimethoxyphenyl)thiophene (3):** Compound **3** was prepared according to the same procedure as **2** with 1-bromo-2,5-dimethoxybenzene (13.8 mmol, 2.99 g), 2-(tributylstannyl)thiophene (13.8 mmol, 5.149 g), bis(triphenylphosphane)dichloropalladium (194 mg, 2 mol-%) and triphenylphosphane (579 mg, 2.21 mmol). After the reaction, the crude product was purified over a chromatographic silica gel column (pentane/diethyl ether, 90:10) to give **3** as a pale yellow oil in 90% yield (2.735 g). <sup>1</sup>H NMR (200 MHz, CDCl<sub>3</sub>): δ = 7.49 (dd, *J* = 3.7, *J* = 1.3 Hz, 1 H, H<sub>Th</sub>), 7.32 (dd, *J* = 5.1, *J* = 1.3 Hz, 1 H, H<sub>Th</sub>), 7.22 (d, *J* = 2.8 Hz, 1 H, H<sub>Ph</sub>), 7.09 (dd, *J* = 5.1, *J* = 3.7 Hz, 1 H, H<sub>Th</sub>), 6.92 (d, *J* = 10 Hz, 1 H, H<sub>Ph</sub>), 6.81 (dd, *J* = 10, *J* = 2.8 Hz, H<sub>Ph</sub>), 3.84 (s, 3 H, H<sub>OMe</sub>), 3.78 (s, 3 H, H<sub>OMe</sub>) ppm. <sup>13</sup>C NMR (200 MHz, CDCl<sub>3</sub>): δ = 143.4 (C<sub>Th</sub>), 135.4 (C<sub>Ph</sub>), 134.0 (C<sub>Ph</sub>), 133.0 (C<sub>Ph</sub>), 130.9 (C<sub>Th</sub>), 130.7 (C<sub>Th</sub>), 128.9 (C<sub>Th</sub>), 127.9 (C<sub>Ph</sub>), 126.3 (C<sub>Ph</sub>), 125.0 (C<sub>Ph</sub>), 20.6 (C<sub>Me</sub>), 20.7 (C<sub>Me</sub>) ppm. IR (KBr): ν̄ = 3082, 2996, 2944, 2826, 1609, 1576, 1473, 1355, 1285, 1222, 1041, 831, 798, 695, 618 cm<sup>-1</sup>. MS (FAB<sup>+</sup>): *m/z* (%) = 220 (100) [M]<sup>+</sup>, 205 (90) [M - 15]<sup>+</sup>, 177 (10), 162 (10), 134 (10). Absorption (CHCl<sub>3</sub>): λ<sub>max</sub> = 325 nm. C<sub>12</sub>H<sub>12</sub>O<sub>2</sub>S (220.29): calcd. C 65.42, H 5.49; found C 65.63, H 5.71.

**1,4-Di(2-thienyl)benzene (4):** Compound **4** was prepared according to the same procedure as **2** with 1,4-dibromobenzene (16 mmol, 3.84 g), 2-tributylstannylthiophene (32 mmol, 11.95 g), bis(triphenylphosphane)dichloropalladium (224 mg, 2 mol-%) and triphenylphosphane (672 mg). After the reaction, the crude product was purified by recrystallisation from ethanol/CH<sub>2</sub>Cl<sub>2</sub> (95:5) to give **4** as a yellow solid in 80% yield (2.405 g). M.p. 206 °C. <sup>1</sup>H NMR (200 MHz, CDCl<sub>3</sub>): δ = 7.58 (s, 4 H, H<sub>Ph</sub>), 7.28 (dd, *J* = 3.6, *J* = 1.2 Hz, 2 H, H<sub>Th</sub>), 7.23 (dd, *J* = 5.1, *J* = 1.2 Hz, 2 H, H<sub>Th</sub>), 7.02 (dd, *J* = 5.1, *J* = 3.6 Hz, 2 H, H<sub>Th</sub>) ppm. <sup>13</sup>C NMR (200 MHz, CDCl<sub>3</sub>): δ = 143.9 (C<sub>Th</sub>), 135.1 (C<sub>Th</sub>), 129.4 (C<sub>Th</sub>), 128.1 (C<sub>Th</sub>), 125.7 (C<sub>Ph</sub>), 123.5 (C<sub>Ph</sub>) ppm. IR (KBr): ν̄ = 3088, 3066, 3031, 1589, 1492, 1427 1265, 1110, 1056, 958, 852, 814, 696 cm<sup>-1</sup>. MS: *m/z* (%) = 242 (55) [M]<sup>+</sup>, 154 (100), 137 (100). Absorption (CHCl<sub>3</sub>): λ<sub>max</sub> = 325 nm.

The spectroscopic data agree with those reported in the literature.<sup>[9]</sup>

**1,4-Dimethyl-2,5-di(2-thienyl)benzene (5):** Compound **5** was prepared according to the same procedure as **2** with 1,4-dibromo-2,5-dimethylbenzene (16 mmol, 4.22 g), 2-(tributylstannyl)thiophene (32 mmol, 11.95 g), bis(triphenylphosphane)dichloropalladium (224 mg, 2 mol-%) and triphenylphosphane (672 mg). After the reaction, the crude product was purified over a chromatographic silica gel column (pentane/diethyl ether, 90:10) to give **5** as a white solid in 75% yield (3.24 g). <sup>1</sup>H NMR (200 MHz, CDCl<sub>3</sub>): δ = 7.38–7.35 (m, 4 H), 7.14–7.12 (m, 4 H), 2.47 (s, 6 H, Me) ppm. <sup>13</sup>C NMR (200 MHz, CDCl<sub>3</sub>): δ = 134.0 (C<sub>Th</sub>), 133.8 (C<sub>Ph</sub> = C<sup>1</sup> and C<sup>4</sup>), 133.2 (C<sub>Ph</sub> = C<sup>2</sup> and C<sup>5</sup>), 133.1 (C<sub>Ph</sub> = C<sup>3</sup> and C<sup>6</sup>), 127.6 (C<sub>Th</sub>), 126.9 (C<sub>Th</sub>), 125.6 (C<sub>Th</sub>), 21.0 (C<sub>Me</sub>) ppm. IR (KBr): ν̄ = 3069, 3005, 2952, 2919, 2857, 1490, 1451, 1432, 1379, 1040, 1032, 957,

892, 829, 701  $\text{cm}^{-1}$ . MS (FAB+):  $m/z$  (%) = 270 (100)  $[\text{M}]^+$ , 255 (40)  $[\text{M} - \text{CH}_3]^+$ . Absorption ( $\text{CHCl}_3$ ):  $\lambda_{\text{max}} = 294 \text{ nm}$ .

The spectroscopic data agree with those reported in the literature.<sup>[9]</sup>

**1,4-Dimethoxy-2,5-di(2-thienyl)benzene (6):** Compound **6** was prepared according to the same procedure as **2** with 1,4-dibromo-2,5-dimethoxybenzene (16 mmol, 4.73 g), 2-(tributylstannyl)thiophene (32 mmol, 11.95 g), bis(triphenylphosphane)dichloropalladium (224 mg, 2 mol-%) and triphenylphosphane (672 mg). After the reaction, the crude product was purified over a chromatographic silica gel column (pentane/diethyl ether, 90:10) to give **6** as a white solid in 76% yield (3.67 g). M.p. 135–136 °C.  $^1\text{H}$  NMR (200 MHz,  $\text{CDCl}_3$ ):  $\delta = 7.55$  (dd,  $J = 3.7$ ,  $J = 1.3$  Hz, 2 H,  $\text{H}_{\text{Th}}$ ), 7.36 (dd,  $J = 5.2$ ,  $J = 1.2$  Hz, 2 H,  $\text{H}_{\text{Th}}$ ), 7.26 (s, 2 H,  $\text{H}_{\text{Ph}}$ ), 7.12 (dd,  $J = 5.2$ ,  $J = 3.6$  Hz, 2 H,  $\text{H}_{\text{Th}}$ ), 3.95 (s, 6 H, MeO) ppm.  $^{13}\text{C}$  NMR (200 MHz,  $\text{CDCl}_3$ ):  $\delta = 150.1$  ( $\text{C}_{\text{Ph}}$ ), 139.2 ( $\text{C}_{\text{Th}}$ ), 127.0 ( $\text{C}_{\text{Th}}$ ), 125.8 ( $\text{C}_{\text{Th}}$ ), 125.6 ( $\text{C}_{\text{Th}}$ ), 123.1 ( $\text{C}_{\text{Ph}}$ ), 112.4 ( $\text{C}_{\text{Ph}}$ ), 56.4 ( $\text{C}_{\text{Me}}$ ) ppm. IR (KBr):  $\tilde{\nu} = 3092$ , 3065, 2993, 2964, 2940, 2872, 2829, 1534, 1488, 1462, 1454, 1393, 1290, 1217, 1171, 1062, 1038, 843, 815, 760, 700  $\text{cm}^{-1}$ . MS (FAB+):  $m/z$  (%) = 302 (100)  $[\text{M}]^+$ , 154 (95), 136 (60). Absorption ( $\text{CHCl}_3$ ):  $\lambda_{\text{max}} = 358 \text{ nm}$ .

The spectroscopic data agree with those reported in the literature.<sup>[9]</sup>

**2,5-Dimethoxyphenol:** This compound was prepared according to the literature.<sup>[11]</sup>

**1-Benzoyloxy-2,5-dimethoxybenzene (8):** In a round-bottomed flask, 2,5-dimethoxyphenol (3 g, 19.4 mmol, 1 equiv.), benzyl bromide (3.3 g, 19.4 mmol, 1 equiv.) and potassium carbonate (4 g, 29 mmol, 1.5 equiv.) were refluxed in acetonitrile (100 mL) for 3 h. After cooling and filtration of the potassium carbonate, the solvent was removed in vacuo and the residue was dissolved in dichloromethane. The organic phase was washed with water, dried with sodium sulfate and concentrated. A white solid precipitated and, after washing with pentane, **8** was obtained in 93% yield (4.4 g). M.p. 36 °C.  $^1\text{H}$  NMR (200 MHz,  $\text{CDCl}_3$ ):  $\delta = 7.50$ – $7.25$  (m, 5 H,  $\text{H}_{\text{Ph}}$ ), 6.82 (d,  $J = 8.8$  Hz, 1 H,  $\text{H}^6$ ), 6.53 (d,  $J = 2.7$  Hz, 1 H,  $\text{H}^3$ ), 6.42 (dd,  $J = 8.8$ ,  $J = 2.7$  Hz, 1 H,  $\text{H}^5$ ), 5.13 (s, 2 H,  $\text{OCH}_2\text{Ph}$ ), 3.83 (s, 3 H, MeO), 3.72 (s, 3 H, MeO) ppm.  $^{13}\text{C}$  NMR (200 MHz,  $\text{CDCl}_3$ ):  $\delta = 154.1$  ( $\text{C}^2$ ), 149.2 ( $\text{C}^1$ ), 144.0 ( $\text{C}^3$ ), 137 ( $\text{C}_{\text{Ph}}$ ), 129 ( $\text{C}_{\text{Ph}}$ ), 128 ( $\text{C}_{\text{Ph}}$ ), 127 ( $\text{C}_{\text{Ph}}$ ), 113 ( $\text{C}_{\text{Ph}}$ ), 104 ( $\text{C}_{\text{Ph}}$ ), 103 ( $\text{C}_{\text{Ph}}$ ), 71 ( $\text{OCH}_2\text{Ph}$ ), 55.7 ( $\text{C}_{\text{Me}}$ ), 55.5 ( $\text{C}_{\text{Me}}$ ) ppm.

The spectroscopic data agree with those reported in the literature.<sup>[12]</sup>

**1-Benzoyloxy-2,5-dimethoxy-4-(2-thienyl)benzene (7):** In a round-bottomed flask, **8** (3.2 g, 13 mmol, 1 equiv.), *N*-iodosuccinimide (3.3 g, 14.7 mmol, 1.1 equiv.) and trifluoroacetic acid (0.5 g, 4 mmol, 0.3 equiv.) were diluted in acetonitrile (100 mL) and vigorously stirred for 12 h. Subsequently, the solvent was evaporated and the medium was dissolved in dichloromethane. The organic phase was washed a sodium hydroxide solution (1 N), dried with sodium sulfate and concentrated to give 1-benzoyloxy-2,5-dimethoxy-4-iodobenzene as a yellow powder in 86% yield (4.1 g). This product was used in the next step without further purification.  $^1\text{H}$  NMR (200 MHz,  $\text{CDCl}_3$ ):  $\delta = 7.50$ – $7.30$  (m, 5 H,  $\text{H}_{\text{Ph}}$ ), 7.23 (s, 1 H,  $\text{H}_{\text{Ph}}$ ), 6.49 (s, 1 H,  $\text{H}_{\text{Ph}}$ ), 5.15 (s, 2 H,  $\text{CH}_2$ ), 3.83 (s, 3 H, MeO), 3.72 (s, 3 H, MeO) ppm.

Under nitrogen, 1-benzoyloxy-4-iodo-2,5-dimethoxybenzene (4 g, 1 equiv., 10.8 mmol), 2-thiopheneboronic acid (1.65 g, 1.2 equiv., 12.9 mmol) and  $\text{Na}_2\text{CO}_3$  (2.3 g, 2 equiv., 21.6 mmol) were introduced into a Schlenk tube containing bis(dibenzylideneacetone) palladium (200 mg, 3.2 mol-%) and triphenylphosphane (225 mg, 8 mol-%). The mixture was heated at 60 °C whilst stirring for 12 h.

After cooling, THF was removed and the medium diluted with dichloromethane. The organic phase was washed several times with water, dried with sodium sulfate and concentrated in vacuo to give a black oil purified over a chromatographic silica gel column eluted with a pentane/diethyl ether mixture (90:10). Compound **7** was obtained as a white solid in 71% yield (2.5 g). M.p. 89 °C.  $^1\text{H}$  NMR (200 MHz,  $\text{CDCl}_3$ ):  $\delta = 7.78$  (s, 1 H,  $\text{H}_{\text{Th}} = \text{H}^5$ ), 7.50–7.25 (m, 7 H,  $\text{OCH}_2\text{Ph} + 2\text{H}_{\text{Th}}$ ), 7.06 (m, 1 H,  $\text{H}_{\text{Ph}} = \text{H}^3$ ), 6.59 (s, 1 H,  $\text{H}_{\text{Ph}} = \text{H}^6$ ), 5.19 (s, 2 H,  $\text{OCH}_2\text{Ph}$ ), 3.89 (s, 3 H, MeO), 3.77 (s, 3 H, MeO) ppm.  $^{13}\text{C}$  NMR (200 MHz,  $\text{CDCl}_3$ ):  $\delta = 150.1$  ( $\text{C}^1$ ), 148.2 ( $\text{C}^5$ ), 144.1 ( $\text{C}^2$ ), 139.4 ( $\text{C}_{\text{Ph}}$ ), 136.9 ( $\text{C}_{\text{Th}}$ ), 128.6 ( $2\text{C}_{\text{Ph}}$ ), 128.0 ( $\text{C}_{\text{Th}}$ ), 127.4 ( $\text{C}_{\text{Ph}}$ ), 126.7 ( $\text{C}_{\text{Th}}$ ), 124.6 ( $\text{C}_{\text{Ph}}$ ), 124.4 ( $\text{C}_{\text{Ph}}$ ), 116.1 ( $\text{C}^4$ ), 113.0 ( $\text{C}^3$ ), 101.3 ( $\text{C}^6$ ), 71.5 ( $\text{OCH}_2\text{Ph}$ ), 56.9 ( $\text{C}_{\text{Me}}$ ), 56.5 ( $\text{C}_{\text{Me}}$ ) ppm. IR (KBr):  $\tilde{\nu} = 3069$ , 1608, 1212, 760  $\text{cm}^{-1}$ . HRMS (FAB+): calcd. for  $\text{C}_{19}\text{H}_{18}\text{O}_3\text{S}$  326.0976; found 326.0975.

### Theoretical Section

Calculations were performed with the Gaussian 98 program<sup>[30,31]</sup> using the density functional theory method.<sup>[32]</sup> The various structures were fully optimised at the B3LYP level.<sup>[33]</sup> This functional was built using Becke's three-parameter exchange functional<sup>[34a]</sup> and the Lee–Yang–Parr correlation functional.<sup>[33c]</sup> The 6-31G(d,p) basis set was used. All atoms were augmented with a single set of polarisation functions. Several publications have shown that the hybrid functional B3LYP is adequate for studying the electronic structures of  $\pi$ -conjugated systems such as those involving a phosphole moiety,<sup>[34]</sup> EDOT<sup>[35]</sup> or  $\pi$ -conjugated oligomers.<sup>[36]</sup>

Second derivatives were calculated in order to check that the optimised structures are true minima on the potential energy surface. All total energies have been zero-point-energy (ZPE) and temperature-corrected using unscaled density functional frequencies.

NBO population analysis<sup>[37]</sup> was performed in order to determine the total charges for each atom and to check if strong or weak stabilising interactions between a filled orbital and an empty orbital exist for the studied systems.

Ionisation energies<sup>[38]</sup> were calculated as suggested previously by Stowasser and Hoffmann.<sup>[39]</sup> Other authors, like Arduengo and co-workers<sup>[40]</sup> or Werstuijk and Rademacher and their co-workers,<sup>[41]</sup> used this method in order to assign different PE spectra.

Molecular orbital diagrams were plotted using the MOLEKEL package.<sup>[42]</sup>

### X-ray Crystal Structure Determinations

Crystals were selected and inserted inside thin-wall Lindemann capillaries for X-ray diffraction analyses. The best diffracting single crystals were used for data collection at 173 K. Diffracted intensities were measured over a full sphere of the reciprocal space on an Xcalibur CCD (Oxford Diffraction) diffractometer using monochromated Mo- $K_\alpha$  radiation ( $\lambda = 0.71073 \text{ \AA}$ ). CrysAlisCCD and CrysAlisRed software packages<sup>[43]</sup> were used for data acquisition, extraction and reduction. The structures were solved using the direct methods provided by SHELXS-97<sup>[44]</sup> and subsequent Fourier analyses. Refinement of atomic positions and anisotropic displacement parameters for all non-hydrogen atoms were carried out by the full-matrix least-squares method based on  $F^2$  (program SHELXL-97<sup>[45]</sup>). Hydrogen atoms attached to carbon were placed in geometrically idealised positions and constrained to ride on their parent atoms. They were given an isotropic displacement parameter equal to 1.2 times the  $U_{\text{eq}}$  of their C parent.

**Crystal Data for 6:**  $\text{C}_{16}\text{H}_{14}\text{O}_2\text{S}_2$ ,  $M = 302.39$ , monoclinic, space group  $P2_1/c$ ,  $a = 11.212(1)$ ,  $b = 7.586(1)$ ,  $c = 18.723(1) \text{ \AA}$ ,  $\beta = 116.34(2)^\circ$ ,  $V = 1427.1(2) \text{ \AA}^3$ ,  $T = 173 \text{ K}$ ,  $Z = 4$ ,  $D_c = 1.407 \text{ g cm}^{-3}$ ,

yellow,  $0.31 \times 0.38 \times 0.47$  mm,  $\mu = 0.37$  mm<sup>-1</sup>, 25658 reflections measured ( $2\theta_{\max} = 64^\circ$ ), 4647 unique,  $R_{\text{int}} = 0.133$ . Final  $R_1 = 0.0566$  and  $wR_2 = 0.1483$  for 181 refined parameters and 1885 observed data points with  $I > 3\sigma(I)$ . Goodness of fit = 0.912, electron density residuals  $0.31/-0.38$  eÅ<sup>-3</sup>.

**Crystal Data for 7:** C<sub>19</sub>H<sub>18</sub>O<sub>3</sub>S,  $M = 326.39$ , orthorhombic, space group  $P2_12_12_1$ ,  $a = 5.3220(5)$ ,  $b = 8.5420(5)$ ,  $c = 35.178(2)$  Å,  $V = 1599.2(2)$  Å<sup>3</sup>,  $T = 173$  K,  $Z = 4$ ,  $D_c = 1.356$  g cm<sup>-3</sup>, colourless,  $0.21 \times 0.33 \times 0.65$  mm,  $\mu = 0.21$  mm<sup>-1</sup>, 20675 reflections measured ( $2\theta_{\max} = 50^\circ$ ), 2815 unique,  $R_{\text{int}} = 0.082$ . Flack parameter = 0.04(1). Final  $R_1 = 0.0549$  and  $wR_2 = 0.1163$  for 211 refined parameters and 2726 observed data points with  $I > 2\sigma(I)$ . Goodness of fit = 1.074, electron density residuals =  $0.25/-0.27$  eÅ<sup>-3</sup>.

CCDC-616271 (for 7) and -616272 (for 6) contain the supplementary crystallographic data for this paper. These data can be obtained free of charge from The Cambridge Crystallographic Data Centre via [www.ccdc.cam.ac.uk/data\\_request/cif](http://www.ccdc.cam.ac.uk/data_request/cif).

**Supporting Information** (see also the footnote on the first page of this article): Structural and electronic properties of the rotamers, full description of the PE spectra and Z-matrix.

## Acknowledgments

The authors gratefully acknowledge financial support from the "Ministère de la Recherche" and the Centre National de la Recherche Scientifique (CNRS). We thank the Institut du Développement de Ressources en Informatique Scientifique (IDRIS, Orsay, France), administered by the CNRS, for the use of calculation facilities and Dr Pfister-Guillouzo for fruitful discussions.

- [1] J. R. Sheats, H. Antoniadis, M. Hueschen, W. Leonard, J. Miller, R. Moon, D. Roitman, A. Stocking, *Science* **1996**, *273*, 884–888.
- [2] a) T. A. Stockheim, R. L. Elsenbaumer, J. R. Reynolds (Eds.), *Handbook of Conducting Polymers*, Marcel Dekker, New York, **1998**; b) H. S. Nalwa (Ed.), *Handbook of Organic Conductive Molecules and Polymers*, vol. 1–3, John Wiley & Sons, New York, **1997**.
- [3] R. D. Mc Cullough, P. C. Ewbank in *Handbook of Conducting Polymers* (Eds.: T. A. Stockheim, R. L. Elsenbaumer, J. R. Reynolds), Marcel Dekker, New York, **1998**, chapter 9, pp. 225–258.
- [4] H. Sirringhaus, P. J. Brown, R. H. Friend, M. M. Nielsen, K. Bechgaard, B. M. W. Langeveld-Voss, A. J. H. Spiering, R. A. J. Janssen, E. W. Meijer, P. Herwig, D. M. De Leeuw, *Nature* **1999**, *401*, 685–687.
- [5] J.-P. Lère-Porte, J. J. E. Moreau, F. Serein-Spirau, C. Torrelilles, A. Righi, J.-L. Sauvajol, M. Brunet, *J. Mater. Chem.* **2000**, *10*, 927–932.
- [6] R. A. Silva, F. Serein-Spirau, M. Bouachrine, J.-P. Lère-Porte, J. J. E. Moreau, *J. Mater. Chem.* **2004**, *14*, 3043–3050.
- [7] a) S. Hotta, S. A. Lee, *Synth. Met.* **1999**, *101*, 551–552; b) S. Hotta, S. A. Lee, T. Tamaki, *J. Heterocycl. Chem.* **2000**, *37*, 25–29; c) S. Hotta, S. A. Lee, H. Kimura, *J. Heterocycl. Chem.* **2000**, *37*, 25–29.
- [8] a) M. Mushrush, A. Fchetti, M. Lefenfeld, H. E. Katz, T. J. Marks, *J. Am. Chem. Soc.* **2003**, *125*, 9414–9423; b) A. Fchetti, J. Letizia, M.-H. Yoon, M. Mushrush, H. E. Katz, T. J. Marks, *Chem. Mater.* **2004**, *16*, 4715–4727.
- [9] A. Pelter, I. Jenkins, D. Jones, *Tetrahedron* **1997**, *53*, 10357–10400.
- [10] F. Alonso, M. Yus, *Tetrahedron* **1991**, *47*, 313–316.
- [11] U. Wriede, M. Fernandez, K. F. West, D. Harcourt, H. W. Moore, *J. Org. Chem.* **1987**, *52*, 4485–4489.
- [12] T. Capecchi, C. B. de Koning, J. P. Michael, *J. Chem. Soc. Perkin Trans. 1* **2000**, 2681–2688.
- [13] A.-S. Castanet, F. Colobert, P.-E. Broutin, *Tetrahedron Lett.* **2002**, *43*, 5047–5048.
- [14] a) M. Turbiez, P. Frère, J. Roncali, *J. Org. Chem.* **2003**, *68*, 5357–5360; b) M. Turbiez, P. Frère, M. Allain, C. Videtot, J. Ackermann, J. Roncali, *Chem. Eur. J.* **2005**, *11*, 3742–3752; c) I. F. Perepichka, S. Roquet, P. Leriche, J.-M. Raimundo, P. Frère, J. Roncali, *Chem. Eur. J.* **2006**, *12*, 2960–2966; d) A. Dkhissi, F. Louwet, L. Groenendaal, D. Beljonne, R. Lazzaroni, J. L. Brédas, *Chem. Phys. Lett.* **2002**, *359*, 466–472.
- [15] F. T. Burling, B. M. Goldstein, *J. Am. Chem. Soc.* **1992**, *114*, 2313–2320.
- [16] Y. Nagao, T. Honjo, H. Iimori, S. Goto, S. Sano, M. Shiro, K. Yamaguchi, Y. Sei, *Tetrahedron Lett.* **2004**, *45*, 8757–8761.
- [17] K. M. Kim, Y.-A. Lee, O.-S. Jung, Y. S. Sohn, *Bull. Korean Chem. Soc.* **1996**, *17*, 93–95.
- [18] M. Pomerantz, A. S. Amarasekara, H. V. R. Dias, *J. Org. Chem.* **2002**, *67*, 6931–6937.
- [19] a) M. Turbiez, P. Frère, P. Blanchard, J. Roncali, *Tetrahedron Lett.* **2000**, *41*, 5521–5525; b) J.-M. Raimundo, P. Blanchard, P. Frère, N. Mercier, I. Ledoux-Rak, R. Hierle, J. Roncali, *Tetrahedron Lett.* **2001**, *42*, 1507–1510.
- [20] J.-F. Pan, S.-J. Chua, W. Huang, *Chem. Phys. Lett.* **2002**, *363*, 18–24.
- [21] See for example: a) J. W. Rabalais, *Principles of Ultraviolet Photoelectron Spectroscopy*, John Wiley & Sons, New York, **1977**; b) U. Lottermoser, P. Rademacher, M. Mazik, K. Kowski, *Eur. J. Org. Chem.* **2005**, 522–531; c) P. Rademacher, *Chem. Rev.* **2003**, *103*, 933–976.
- [22] C. N. R. Rao, P. K. Basu, M. S. Hegde, *Systematic Organic UV Photoelectron Spectroscopy*, Marcel Dekker, New York, **1979**.
- [23] See for example: H. Bock, B. Roth, *Phosphorus Sulfur* **1983**, *14*, 211–223.
- [24] a) J.-J. Yeh, *Atomic Calculation of Photoionisation Cross-Sections and Asymmetry Parameters*, Gordon and Breach Science Publishers, Langhorne, PE, **1993**; b) I. P. Csonka, G. Vass, L. Szepes, D. Szabo, I. Kapovits, *J. Mol. Struct. (THEOCHEM)* **1998**, *455*, 141–159.
- [25] V. I. Minkin, R. M. Minyaev, *Mendeleev Commun.* **2000**, *5*, 167–206.
- [26] G. D. Markham, C. W. Bock, *J. Mol. Struct. (THEOCHEM)* **1997**, *418*, 139–154.
- [27] M. Iwaoka, H. Komatsu, T. Katsuda, S. Tomoda, *J. Am. Chem. Soc.* **2004**, *126*, 5309–5317.
- [28] A. F. Cozzolino, I. Vargas-Baca, S. Mansour, A. H. Mahmoudkhani, *J. Am. Chem. Soc.* **2005**, *127*, 3184–3190.
- [29] J. Wolfe, R. Singer, B. Yang, S. Buchwald, *J. Am. Chem. Soc.* **1999**, *121*, 9550–9561.
- [30] M. J. Frisch, G. W. Trucks, H. B. Schlegel, G. E. Scuseria, M. A. Robb, J. R. Cheeseman, V. G. Zakrzewski, J. A. Montgomery, R. E. Stratman, J. C. Burant, S. Dapprich, J. M. Millam, A. D. Daniels, K. N. Kudin, M. C. Strain, O. Farkas, J. Tomasi, V. Barone, M. Cossi, R. Cammi, B. Mennucci, C. Pomelli, C. Adamo, S. Clifford, J. Ochterski, G. A. Petersson, P. Y. Ayala, Q. Cui, K. Morokuma, D. K. Malick, A. D. K. Rabuck, K. Raghavachari, J. B. Foresman, J. Cioslowski, J. V. Ortiz, A. G. Baboul, B. B. Stefanov, G. Liu, A. Liashenko, P. Piskorz, I. Komaromi, R. Gomperts, R. Martin, D. J. Fox, T. Keith, M. A. Al-Laham, C. Y. Peng, A. Nanayakkara, C. Gonzalez, M. Challacombe, P. M. W. Gill, B. Johnson, W. Chen, M. W. Wong, J. L. Andres, M. Head-Gordon, E. S. Replogle, J. A. Pople, *Gaussian 98, Revision A.7*, Gaussian, Inc., Pittsburgh, PA, **2001** (A.11.1) or **2002** (A.11.3).
- [31] W. J. Hehre, L. Radom, P. v. R. Schleyer, J. A. Pople, *Ab initio Molecular Orbital Theory*, John Wiley & Sons, New York, **1986**.
- [32] R. G. Parr, W. Yang, *Functional Theory of Atoms and Molecules* (Eds.: R. Breslow, J. B. Goodenough), Oxford University Press, New York, **1989**.

- [33] a) A. D. Becke, *Phys. Rev. A* **1988**, *38*, 3098–3100; b) A. D. Becke, *J. Chem. Phys.* **1993**, *98*, 5648–5652; c) C. Lee, W. Yang, R. G. Parr, *Phys. Rev. B* **1988**, *37*, 785–789.
- [34] a) M. A. De Oliveira, H. F. Dos Santos, W. B. De Almeida, *Phys. Chem. Chem. Phys.* **2000**, *2*, 3373–3380; b) D. Delaere, M. T. Nguyen, L. G. Vanquickenborne, *J. Phys. Chem. A* **2003**, *107*, 838–846.
- [35] D. Delaere, M. T. Nguyen, L. G. Vanquickenborne, *J. Phys. Chem. A* **2003**, *107*, 838–846.
- [36] P. Blanchard, P. Verlhac, L. Michaux, P. Frère, J. Roncali, *Chem. Eur. J.* **2006**, *12*, 1244–1255.
- [37] a) A. E. Reed, L. A. Curtiss, F. Weinhold, *J. Chem. Rev.* **1988**, *88*, 899–926; b) J. P. Foster, F. Weinhold, *J. Am. Chem. Soc.* **1980**, *102*, 7211–7218.
- [38] Estimated IPs (except for  $IP_1$ ) were calculated by applying a uniform shift at the different Kohn–Sham energies [shift:  $x = IP_1^{exp} + \epsilon^{KS}(\text{HOMO})$ ], where  $\epsilon^{KS}(\text{HOMO})$  is the highest occupied B3LYP/6-31G\*\* Kohn–Sham MO energy of the ground-state molecule and  $IP_1^{exp}$  is the lowest experimental IP of the molecule, as suggested previously by Stowasser and Hoffmann.<sup>[39]</sup> The first estimated IP is taken to be equal to the first experimental ionisation potential.
- [39] R. Stowasser, R. Hoffmann, *J. Am. Chem. Soc.* **1999**, *121*, 3414–3420.
- [40] A. J. Arduengo III, H. Bock, H. Chen, M. Denk, D. A. Dixon, J. C. Green, W. A. Hermann, N. L. Jones, M. Wagner, R. West, *J. Am. Chem. Soc.* **1994**, *116*, 6641–6649.
- [41] a) H. M. Muchall, P. Rademacher, *J. Mol. Struct.* **1997**, *435*, 157–167; b) H. M. Muchall, P. Rademacher, *J. Mol. Struct.* **1998**, *471*, 189–194; c) H. M. Muchall, N. H. Werstiuk, B. Choudhury, *Can. J. Chem.* **1998**, *76*, 221–227; d) H. M. Muchall, N. H. Werstiuk, B. Choudhury, J. Ma, J. Warkentin, J. P. Pezacki, *Can. J. Chem.* **1998**, *76*, 238–240.
- [42] a) P. F. Flükiger, “Development of the molecular graphics package MOLEKEL and its application to selected problems in organic and organometallic chemistry”, Ph. D. Dissertation, University of Geneva, **1992**; b) *MOLEKEL: An Interactive Molecular Graphics Tool*: S. Portmann, H. P. Lüthi, *Chimia* **2000**, *54*, 766–770.
- [43] *CrysAlisCCD and CrysAlisRed 169 software package*, **2001**, Oxford Diffraction, Ltd., Abingdon, UK.
- [44] G. M. Sheldrick, *SHELXS-97: A Program for Crystal Structures Solution*, **1997**, University of Göttingen, Germany.
- [45] G. M. Sheldrick, *SHELXL-97: A Program for Refining Crystal Structures*, **1997**, University of Göttingen, Germany.

Received: December 21, 2006  
Published Online: June 25, 2007